Substitution Effect of 1,7-Asymmetrically Substituted 3,4:9,10-Perylenebis(dicarboximide) Dyes

B. Sun[a]; Y. Zhao[a]; X. Qiu[a]; C. Han[a]; Y. Yu[a]; Z. Shi[a]

[a] Department of Chemistry, Shandong Normal University, Jinan, People's Republic of China

PLEASE SCROLL DOWN FOR ARTICLE

Substitution Effect of 1,7-Asymmetrically Substituted 3,4:9,10-Perylenebis(dicarboximide) Dyes

B. SUN, Y. ZHAO, X. QIU, C. HAN, Y. YU and Z. SHI*

Department of Chemistry, Shandong Normal University, 88 Wenhuadonglu Road, Jinan 250014, People's Republic of China

1,7-Asymmetrically substituted 3,4:9,10-perylenebis (dicarboximide) dyes (2a, 2b, and 3) with electron donor or acceptor groups have been synthesized in good yields under mild conditions. The electrochemistry and steady-state spectroscopy of these perylene bisimides were discussed. The strong electron donating pyrrolidinyl and electron withdrawing bromine substitutes led to a serious deviation from intrinsic electronic structure of the perylene bisimide core. Furthermore, the packing behaviors in solution were investigated with absorption spectra. These results were in good agreement with the theory calculations at B3LYP/6-31G* level and made them a valuable addition to the family of robust perylene-based chromophores that can be used to develop new photoactive charge transport materials.

Keywords: Perylenebis (dicarboximide); Asymmetrical substitution; Electronic structure; Packing

INTRODUCTION

Owing to their high photochemical stability, ease of synthetic modification, and desirable optical/redox characteristics, perylene-3,4:9,10-bis(dicarboximide) (PBI) and related derivatives continued to receive considerable attention for applications such as field effect transistors [1,2], molecular electronics [3–5], light-harvesting arrays, solar cells [6,7], and light-emitting diodes [8,9]. They also have been proven to be good building blocks for constructing supramolecular or giantmolecular systems [10]. For the preparation of soluble perylene bisimide dyes due to their intrinsic insolubility, two different modification strategies had been developed to improve the solubility in organic solvents. Incorporating soluble substitutes at the imide nitrogen usually exhibits indistinguishable absorption and emission properties because nodes in the HOMO and LUMO at the imide nitrogen reduce the coupling between the perylene bisimide units and the imide substituents to a minimum [11,12]. Introducing substituents at the carbocyclic scaffold in the so-called bay-area is more complicated [13]. Various disubstituted derivatives have been prepared from dibromo-perylene bisimide, such as carbon [14], cyano [15], oxygen [13] and nitrogen [16,17] nucleophiles could be coupled to the perylene core to afford novel perylene bisimide dyes with interesting optical and redox features. In our previous works, the symmetrically 1,7-substituted PBIs with p-tert-butylphenol and pyrrolidine had been synthesized with wonderful yields [18]. However, introduction of different nucleophiles had been proved to be difficult and a reasonable yield was rarely afforded [19]. In this paper, these chromophores are focused on the introduction of different groups (p-tert-butylphenoxy and pyrrolidinyl) at 1 and 7 positions of the 3,4:9,10-perylenebis(dicarboximide) to afford asymmetrical products with high yields and on further understanding the substitution effect in the optical, redox properties and packing behaviour.

RESULTS AND DISCUSSION

Synthesis

The compounds **4a** and **4b** have been well synthesized in good yields by our laboratory and others [16–18,20,21]. In an effort to expand the scope of chromophores available for designing systems for self-assembly and charge transfer based on PBI, mono-substituted **2a**, **2b** and asymmetrically substituted **3**

*Corresponding author. E-mail: zshi@sdnu.edu.cn

were obtained by controlling the reaction condition. The synthesis of perylene bisimide **2a**, **2b** and **3** followed the strategy outlined in Scheme 1. Compound **1** was used as the starting material to synthesize **2a**, **2b** by mono-substitution with p-tert-butylphenol and pyrrolidine respectively. **2a** was prepared in NMP at room temperature in 46% yield. However, the disubstituted product **4a** would be yielded increasingly along with longer reaction time or/and at higher temperature. For the synthesis of **2b**, pyrrolidine could be also used as the solvent, but it was found that disubstituted product **4b** was afforded inevitably accompanying with the mono-substitute product **2b**. When dichloromethane was used as solvent, compound **2b** was afforded as the only product in a yield of 80% at room temperature. Compound **3** was readily synthesized from **2a** by stirring with pyrrolidine at room temperature in a yield reaching to 90%.

Alternatively, **2b** could also be used to synthesize **3**, but the yield was poor (<12%). Those results were attributed to the strong electron-donating effect of pyrrolidinyl group, which increased the electron cloud density on the perylene core and led the less active nucleophile to react difficultly.

B3LYP/6-31G* Calculations

The energy and geometry calculations were performed with Gaussian 03 installed on a Windows PC. The geometries of **2a**, **2b** and **3** were optimized with restricted DFT, incorporating the B3LYP functional and 6-31G basis set. The MO analysis of **2a**, **2b** and **3** showed that the highest occupied MO (HOMO) and the lowest unoccupied MO (LUMO) were localized well in the perylene core. The ground-state geometries calculated at B3LYP/6-31G* level had different
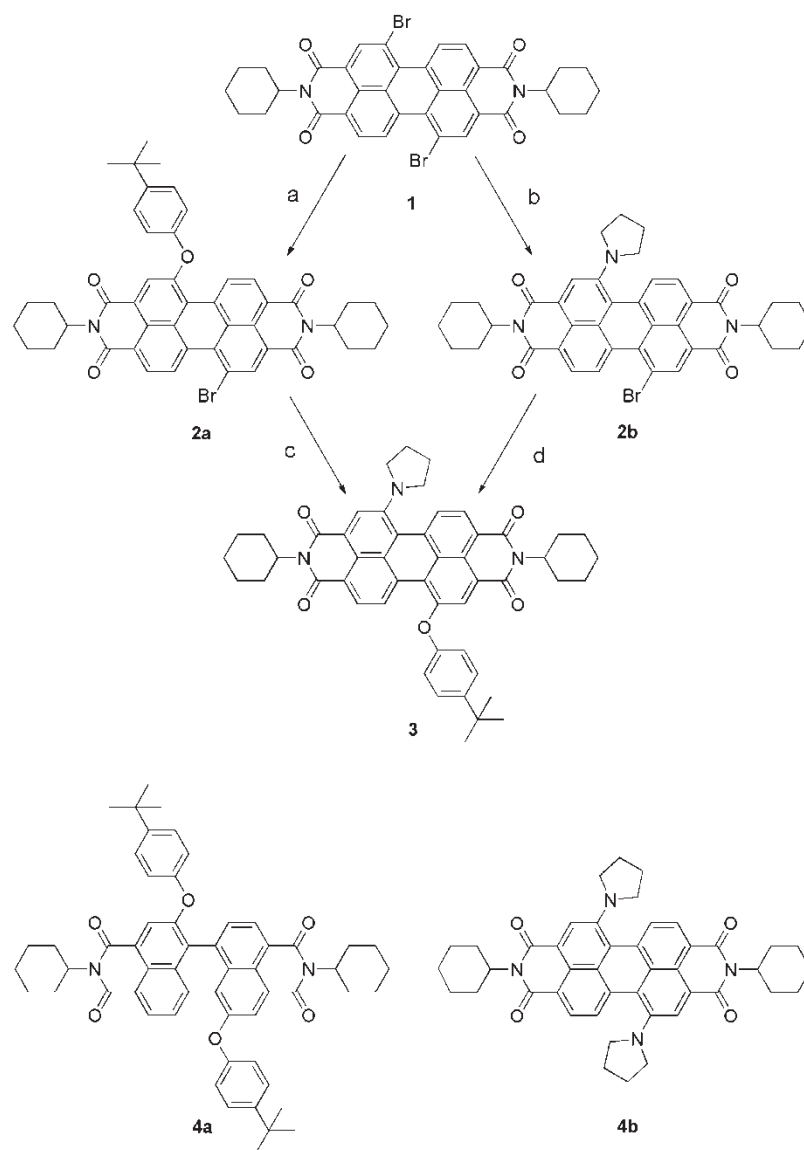
SCHEME 1   Synthetic route of compounds **2a**, **2b**, **3** and the chemical structures of **4a** and **4b**. (a) *p*-tert-butylphenoxy, K$_2$CO$_3$, NMP, rt, 18 h, 46%; (b) pyrrolidine, CH$_2$Cl$_2$, K$_2$CO$_3$, reflux, 3 h, 78%; (c) pyrrolidine, rt, 30 min, 88%; (d) *p*-tert-butylphenoxy, K$_2$CO$_3$, NMP, rt, 30 h, 11.2%.

core twist angles of the perylene core, which were 15.1°, 22.4° and 21.2° for **2a**, **2b** and **3** respectively (Fig. 1). Basically, the pyrrolidinyl substitution resulted in large dihedral twist of PBI core more than 20°.

To more clearly visualize the electronic properties of PBI dyes, electrostatic potential maps were also calculated from B3LYP/6-31G* density functional calculations. The process involved calculation of every part of the electron density cloud of the dyes. The electrostatic potential was then mapped onto an isosurface of the total SCF electron density ($0.0004\,e\text{\AA}^{-3}$ for the map generated in present work). The electrostatic potential map generated via this procedure was then color-coded according to its potential with the regions of most negative electrostatic potential shown in red and those with the most positive electrostatic potential shown in blue. As shown in Fig. 2, the regions with the strongest negative potential (color-coded in red) occurred in the immediate vicinity of the O atom in imide groups. In contrast, the most electropositive regions (color-coded in blue) occurred on the pyrrolidinyl or phenoxy groups substituted. However, the colors were different even for the same substitution groups of different dyes. The pyrrolidinyl group of **2b** was the bluest in dyes of containing pyrrolidinyl groups including **3** and **4b**. Similarly, the phenoxy group of **2a** was the most electropositive among the phenoxy substitutes (**2a**, **4a** and **3**). It was suggested that the presence of strong electron-withdrawing bromine atom could withdraw more electron cloud from the electron-donating groups (p-tert-butylphenoxy or pyrrolidinyl) by transfer through the aromatic perylene core, resulting in the donating group regions becoming more electron-deficient. This result could also be demonstrated by the colors of the bromine atoms of **2a** and **2b** in the electrostatic potential map, which were more yellow

than it displayed in dibromo-PBI **1**. Those indicated that the bromine atom attracted more electron cloud in the presence of electron donor group. As expected, the delocalized π electron clouds of the aromatic cores were extensively affected by the substitution groups. In general, the color of the dibromo-PBI (**1**) core was blue, indicating a fairly electron deficient state. While the dipyrrolidinyl substituted PBI (**4b**) core was yellow, suggesting a large electron density at the core. Comparing the cores of compounds **3**, **2b**, **4a** and **2a**, the colors changed from pale yellow to green. Thus it was assumed that the delocalized π electron density order of the cores was **4b** > **3** > **2b** ≈ **4a** > **2a** > **1**. Accordingly, the first bromine atom of **1** was substituted by pyrrolidinyl or phenoxy group readily owing to the fairly electron deficient of the perylene core. However, the second substitution of bromine was harder than the first one especially for **2b** because of the dramatic increase of the electron density of the perylene core resulting from the electron-donating effect of first substitution. Those were in good agreement with the experimental facts.

Electrochemistry

Electrochemical measurements were performed using an electrochemical workstation. The redox potentials were measured by cyclic voltammetry in dry dichloromethane and referenced to the ferrocene/ferrocinium couple (Fc/Fc^{+}). The working electrode was a platinum disk, the reference electrode was Ag/Ag$_x$O and the counter electrode was a platinum wire. The scan rate was $100\,\text{mV/s}$ with Bu$_4$NPF$_6$ as the supporting electrolyte. All electrochemical experiments were carried out under dry nitrogen atmosphere.

The electrochemical properties of perylene bisimides have been investigated by several groups [2,16,17,21–24]. Their contributions showed that
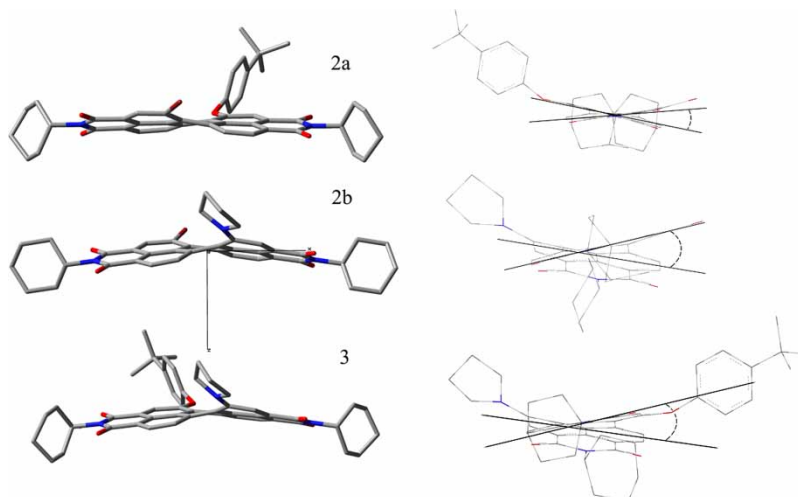

FIGURE 1   DFT (B3LYP/6-31G*) geometry-optimized structures of **2a**, **2b** and **3** shown with view along the short (y) axis (left) and along the long (x) axis (right). For the purposes of the simplified representation, hydrogen atoms are not shown.
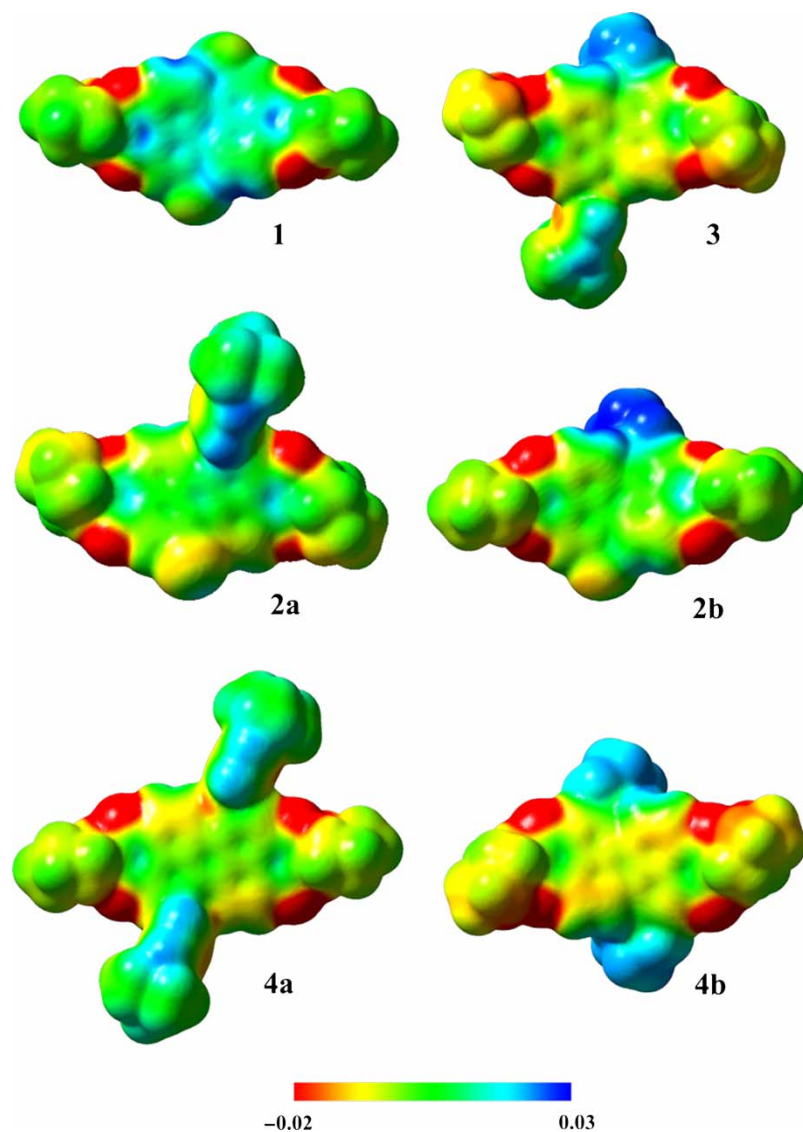
FIGURE 2   Electrostatic potential maps of **1**, **2a**, **2b**, **3**, **4a**, **4b**, the electron rich region is red, the electron poor region is blue.

perylene bisimides were fairly electron deficient dyes, which were easy to reduce and rather difficult to oxidize. For most compounds two reversible reduction and one reversible oxidation waves were found in cyclic voltammetry. In the present work all of the electrochemical one-electron oxidations and reductions of **2a**, **2b**, **3**, **4a** and **4b** were reversible at a platinum electrode. Table I gave the first half-wave potentials for these reactions. From the comparison among these potentials it was found that substitute in the bay-area had a pronounced effect on redox potentials. The reduction potentials varied between -0.74 V and -1.07 V in an order of **2a** > **4a** > **2b** > **3** > **4b**, and the oxidation potentials ranged from 0.66 V to beyond 2.0 V correspondingly in the same order. Based on this, p-tert-butylphenoxy disubstituted **4a** was easier to be reduced and harder to be oxidized than pyrrolidinyl mono-substituted **2b**, suggesting an electron more deficient perylene core of **4a** than that of **2b** despite the presence of strong

electron withdrawing effect of bromine in **2b**. Accordingly, the pyrrolidinyl group had a far stronger tendency to donate electrons than p-tert-butylphenoxy group did. Disubstituted with pyrrolidinyls, **4b** was with the highest reduction potential and the lowest oxidation potential, two reversible oxidation waves were even observed. Those results were consistent with the electrostatic potential maps calculated.

Steady-state Spectroscopy

The influence of substituents on the core could be estimated by quantum chemical calculations and

TABLE I   First half-wave potentials for **2a**, **2b**, **3**, **4a** and **4b**

Compound	**2a**	**2b**	**3**	**4a**	**4b**
$E_{1/2}$(red)	-0.74	-0.85	-1.06	-0.83	-1.07
$E_{1/2}$(ox)	>2.0	1.06	0.90	1.48	0.66

even MO calculations could predict such effect on the absorption of the π-system correctly. A pronounced bathochromic shift was expected if donor groups were attached to the positions 1, 6, 7 and 12 of the 3,4:9,10-perylenebis(dicarboximide)s.

The representative absorption spectra of compounds **2a**, **2b** and **3** in toluene were shown in Fig. 3, in which compounds **4a**, **4b**, and **1** were used as the references to demonstrate the influence of substituted groups. Over 400 nm, compound **2a** showed the PBI core absorption bands with maximum absorption at 533 nm. In the case of compound **2b**, the maximum absorptions appeared at 641 nm. Compared with **1**, the main peaks of p-tert-butylphenoxy or pyrrolidinyl mono-substituted **2a** and **2b** shifted 6 nm and 114 nm respectively. Comparatively, the absorption spectrum of **3** exhibited a similar profile with **2b** with a maximum absorption of 638 nm. Compared with **2a**, the main absorption peak of pyrrolidinyl further substituted **3** was blue-shifted obviously by 105 nm in toluene while that was only 6 nm for phenoxy group further substituted **4a**. A similar trend was found when the bromine atom of **2b** was substituted by p-tert-butylphenoxy or pyrrolidinyl groups to afford compounds **3** or **4b**, which displayed red-shift of 3 nm and 44 nm respectively. These significant differences in absorptions resulted from substitutes indicated that pyrrolidinyl group was a far stronger electron donor than p-tert-butylphenoxy group, which had been demonstrated by calculated results and electrochemistry analysis. Although the characteristic absorption profile of PBIs could be observed for compounds **2b**, **3** and **4b**, their absorption bands underwent a significant band broadening, especially for the longest absorption.

The absorption of the asymmetrically substituted PBIs in different solvents was investigated also (Table II). Compared with the maximum absorption of 522 nm in cyclohexane, the main peak of **2a**
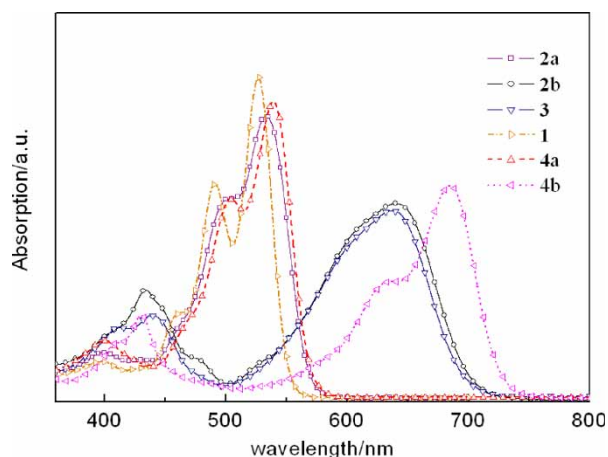
TABLE II λ_{max} (nm) of **2a**, **2b** and **3** in different solvents $(1.0 \times 10^{-5}\,M)$

Compound	Toluene	Chloroform	THF	Cyclohexane
2a	533	540	526	522
2b	641	652	642	621
3	638	648	635	617

red-shifted by 11 nm, 18 nm and 4 nm in toluene, chloroform and tetrahydrofuran (THF) respectively, while the λ_{max} of **2b** and **3** red-shifted corresponding 20 nm, 31 nm, 21 nm and 21 nm, 31 nm, 18 nm respectively. It is proposed that the intense solvent effect of the pyrrolidinyl substitution on absorption was attributed to large molecular polarity owing to presence of pyrrolidinyl group.

Figure 4 showed the fluorescence emission spectra of **2a**, **2b** and **3** in toluene at the same concentration. Compared with compound **1**, the fluorescence intensity of **2a** was slightly decreased in toluene. However, those of pyrrolidinyl incorporated **2b** and **3** were quenching sharply. Similar trends were observed in fluorescence spectra of **4a** and **4b**. This demonstrated that the presence of strong electron-donating groups could dramatically quench the fluorescence of the PBI core. This phenomenon might be attributed to the efficient intramolecular electron transfer from the electron-acceptor perylene bisimide core to the electron-donor groups [25–29].

Packing Behavior of 2a, 2b, and 3 in Solid State and Solution

The π–π interactions of **2a**, **2b** and **3** in toluene were confirmed by UV–vis spectra. For perylene bisimide, the electronic absorption had a pronounced coupling to the vibronic features corresponding to $\upsilon = 0 \rightarrow \upsilon' = 0$, 1, 2 and 3 transitions, where υ and υ' were quantum vibrational numbers of the ground and excited states, respectively. As free monomer,

FIGURE 3 UV–vis spectra of **2a**, **2b**, **3**, **4a**, **4b** and **1** in toluene $(1.0 \times 10^{-5}\,M)$.
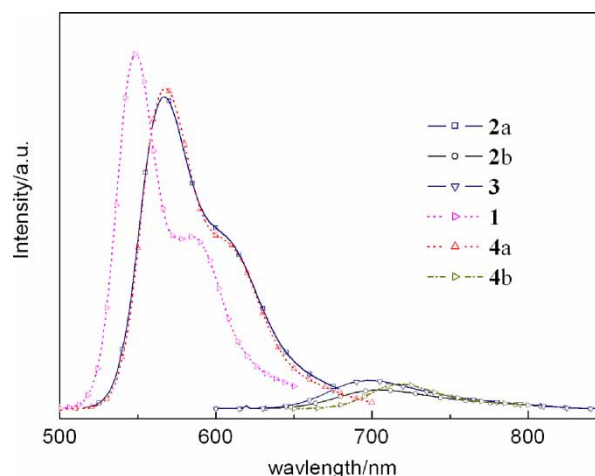

FIGURE 4 Emission spectra of **1**, **2a**, **2b**, **3**, **4a** and **4b** in toluene $(1.0 \times 10^{-5}\,M)$.

normal progression of Franck–Condon factors were $A^{0\rightarrow1} > A^{0\rightarrow2} > A^{0\rightarrow3}$. However, as the monomer began to aggregate, the $0\rightarrow1$ and $0\rightarrow2$ transition increased [30,31]. Figure 5 shows the UV/vis absorption spectra of compound **2a**, **2b** and **3** in concentrations of 10^{-4} M and 10^{-5} M respectively, which were normalized to unity because we were interested in showing the peak shapes. From 10^{-5} M to 10^{-4} M, the $0\rightarrow1$ transition absorption of **2a** increased distinctly in toluene, indicating stronger $\pi-\pi$ interactions occurred in higher concentration. In contrast, no obvious change was observed for the $0\rightarrow1$ transition absorption of **2b** as well as absorption of **3** in different concentrations owing to the big core twist angles of compounds **2b** and **3** decreasing the $\pi-\pi$ interactions.

CONCLUSIONS

In summary, we have described the effective pathway for the synthesis of three 1,7-asymmetrically substituted 3,4:9,10-perylenebis(dicarboximide) dyes (**2a**, **2b**, and **3**). The effects of different substituted groups on the same PBI core were discussed by optical and electrochemical studies, which were in good agreement with the calculation results. The packing behaviors of three asymmetric substituted PBI dyes were investigated in solid state as well as in solution. The strong electron-donating properties of pyrrolidinyl could lead to a serious deviation from intrinsic electronic structures of the PBI cores.

EXPERIMENTAL

Materials

The starting materials, 1,7-dibromo-N,N′-dicyclohexyl-3,4:9,10-perylenebis(dicarboximide) (**1**), disubstitute products 1,7-Bis(p-tert-butylphenoxy)-N,N′-dicyclohexyl perylene-3,4,9,10-tetracarboxylic bisimide (**4a**), and 1,7-Bis (N-pyrrolidinyl)-N,N′-Dicyclohexyl perylene-3,4,9,10-tetracarboxylic bisimide (**4b**) were synthesized according to previous work [18].

1-(p-Tert-butylphenoxy)-7-Bromo-N,N′-Dicyclohexyl-3,4:9,10-Perylenebis(dicarboximide) (2a)

Compound **1** (1.05 g, 1.47 mmol), p-tert-butylphenol (0.26 g, 1.77 mmol), and K_2CO_3 (0.37 g, 2.66 mmol) were stirred in 15 mL N-methyl-2-pyrrolidone (NMP) under argon at room temperature for 18 h (TLC check). The reaction mixture was then poured into 50 mL water. The precipitate was filtered, repeatedly washed with water, and was column chromatographed on silica with 2:1 chloroform/petroleum ether (V:V, R_f = 0.65) to afford a red product 0.58 g (46%). IR (KBr, cm^{-1}): 2927, 2853, 1699, 1659, 1504, 1454, 1402, 1385, 1330, 1261, 1207, 1173, 835, 809, 748, 556. ^{1}H-NMR (300 MHz, CDCl$_3$, ppm): δ 9.61 (d, 1H, J = 8.2 Hz), 9.42 (d, 1H, J = 8.2 Hz), 8.90 (s, 1H), 8.61 (d, 1H, J = 8.2 Hz), 8.60 (d, 1H, J = 8.2 Hz), 8.29 (s, 1H), 7.48 (d, 2H, J = 8.6 Hz), 7.10 (d, 2H, J = 8.6 Hz) 4.99 (m, 2H), 2.53 (m, 4H), 1.89 (m, 4H), 1.74 (m, 6H), 1.37 (m, 6H), 1.25 (s, 9H). ^{13}C-NMR (75 MHz, CDCl$_3$, ppm): δ 163.7, 163.4, 163.0, 156.1, 152.5, 148.6, 138.1, 133.7, 133.1, 132.8, 131.4, 129.4, 128.8, 128.5, 127.6, 127.5, 124.8, 124.7, 123.5, 123.1, 122.7, 119.9, 119.4, 54.3, 34.7, 31.6, 29.3, 29.2, 26.6, 25.5. MS (MALDI): m/z = 780.4 [M]$^+$. Anal. Calcd for C$_{46}$H$_{41}$BrN$_2$O$_5$: C, 70.68; H, 5.29; N, 3.58. Found: C, 70.25; H, 5.03; N, 3.49.

1-(N-Pyrrolidinyl)-7-Bromo-N,N′-Dicyclohexyl-3,4:9,10-Perylenebis(dicarboximide) (2b)

Method A

Compound **1** (1.05 g, 1.47 mmol) was dissolved in 8 mL pyrrolidine, then K_2CO_3 (0.24 g, 1.76 mmol) was added. The solution was stirred at room temperature under dry nitrogen for 8 h. Excess pyrrolidine was removed on a rotary evaporator.
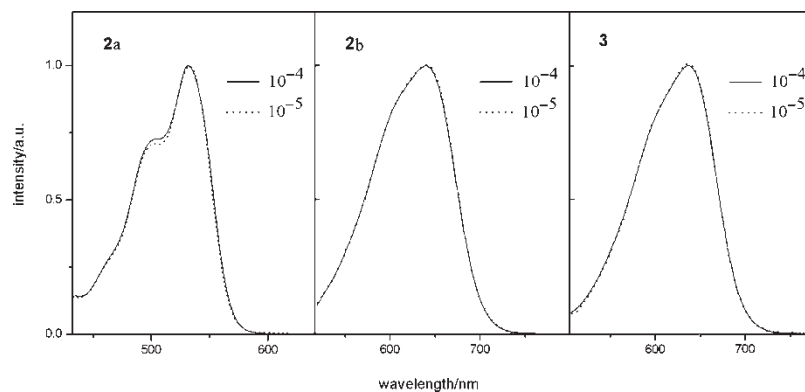

FIGURE 5   Normalized Uv–vis absorption spectra in toluene for compound **2a**, **2b** and **3** (Solid line: 1×10^{-4} M, Dot line: 1×10^{-5} M).

The residue was column chromatographed on silica with 2:1 chloroform/petroleum ether (V:V, R_f = 0.35) to afford a green product (0.39 g, 38%). IR (KBr, cm^{-1}): 2927, 2853, 1693, 1656, 1585, 1418, 1384, 1372, 1328, 1258, 1237, 1188, 1115, 985, 872, 806, 749, 588. ^{1}H-NMR (300 MHz, CDCl$_3$, ppm) δ 9.41 (d, 1H, J = 8.3 Hz), 8.79 (s, 1H), 8.57 (d, 1H, J = 8.0 Hz), 8.47 (s, 1H), 8.41 (d, 1H, J = 8.3 Hz), 7.31 (d, 1H, J = 8.0 Hz), 5.05 (m, 2H), 3.70 (m, 2H), 2.78 (m, 2H), 2.58 (m, 4H) 1.86 (m, 8H), 1.77 (m, 6H), 1.45 (m, 4H), 1.25 (s, 2H). ^{13}C-NMR (75 MHz, CDCl$_3$, ppm) δ 164.3, 164.2, 163.9, 163.2, 148.4, 137.5, 134.6, 134.1, 131.5, 130.0, 129.5, 128.0, 126.4, 125.5, 123.9, 123.5, 122.5, 121.9, 121.7, 121.5, 119.0, 117.3, 115.0, 54.1, 54.0, 53.9, 52.7, 29.2, 26.7, 25.9, 25.6. MS (MALDI): m/z = 701.8 [M]$^+$. Anal. Calcd for C$_{40}$H$_{36}$BrN$_3$O$_4$:C, 68.38; H, 5.16; N, 5.98. Found: C, 68.22; H, 5.03; N, 5.90.

Method B

Compound **1** (1.05 g, 1.47 mmol) and 3 mL pyrrolidine were added to 25 mL dichloromethane. The mixture was heated to reflux under dry nitrogen for 3 h with stirring. The solution was removed on the rotary evaporator and the residue was column chromatographed on silica with chloroform (R_f = 0.56) to afford a green product (0.80 g, 78%).

1-(p-Tert-butylphenoxy)-7-(N-Pyrrolidinyl)-N,N'-Dicyclohexyl-3,4:9,10-Perylenebis(dicarboximide) (3)

Method A

Compound **2b** (1.05 g, 1.49 mmol), p-tert-butylphenol (0.36 g, 2.5 mmol), and K$_2$CO$_3$ (0.37 g, 2.66 mmol) were stirred in 10 mL NMP under argon at room temperature for 28 h (TLC check). The reaction mixture was poured into a solution of water/10%HCl (40/10 mL). The precipitate was filtered, repeatedly washed with water, and dried in a vacuum. The product was column chromatographed on silica with 2:1 chloroform/petroleum ether (V: V, R_f = 0.3) to afford a green product (0.13 g, 11.2%). IR (KBr, cm^{-1}): 2927, 2854, 1693, 1655, 1597, 1506, 1453, 1418, 1384, 1329, 1260, 1238, 1174, 1124, 986, 808, 751, 559. ^{1}H-NMR (300 MHz, CDCl$_3$, ppm) δ 9.38 (d, 1H, J = 8.3 Hz), 8.58 (d, 1H, J = 8.1 Hz), 8.52 (s, 1H), 8.38 (d, 1H, J = 8.3 Hz), 8.29 (s, 1H), 7.62 (d, 1H, J = 8.1 Hz), 7.45 (d, 2H, J = 8.7 Hz), 7.11 (d, 2H, J = 8.7 Hz), 5.05 (m, 2H), 3.77(m, 2H), 2.81 (m, 2H), 2.56 (m, 4H), 2.15 (m, 8H), 1.86 (m, 8H), 1.73 (m, 6H) 1.36 (s, 2H), 1.22 (s, 9H). ^{13}C-NMR (75 MHz, CDCl$_3$, ppm): δ 164.5, 164.4, 164.2, 163.8, 154.3, 153.1, 148.1, 147.9, 135.3, 131.9, 129.5, 128.3, 127.4, 127.1, 125.5, 124.3, 124.0, 123.5, 122.5, 121.6, 119.1, 116.7, 115.1, 54.1, 52.8, 52.5, 34.6, 31.6, 30.2, 29.5, 29.3, 26.7, 25.6. MS (MALDI):

m/z = 771.7 [M]$^+$. Anal. Calcd for C$_{50}$H$_{49}$N$_3$O$_5$: C, 77.80; H, 6.40; N, 5.44. Found: C, 77.59; H, 6.26; N, 5.42.

Method B

Compound **2a** (1.02 g, 1.31 mmol) was dissolved in 8 mL pyrrolidine, then K$_2$CO$_3$ (0.27 g, 1.96 mmol) was added. The solution was stirred at room temperature under dry nitrogen for 30 minute. Excess pyrrolidine was removed on a rotary evaporator and the residue was column chromatographed on silica with 2.5:1 chloroform/petroleum ether (V:V, R_f = 0.55) to afford a green product (0.89 g, 88%).

References

[1] Jones, B. A.; Ahrens, M. J.; Yoon, M. H.; Facchetti, A.; Marks, T. J.; Wasielewski, M. R. *Angew. Chem. Int. Ed.* **2004**, *43*, 6363.

[2] Chen, Z.; Debije, M. G.; Debaerdemaeker, T.; Osswald, P.; Würthner, F. *Chem. Phys. Chem.* **2004**, *5*, 137.

[3] Hayes, R. T.; Wasielewski, M. R.; Gosztola, D. *J. Am. Chem. Soc.* **2000**, *122*, 5563.

[4] Davis, W. B.; Svec, W. A.; Ratner, M. A.; Wasielewski, M. R. *Nature* **1998**, *396*, 60.

[5] Lukas, A. S.; Bushard, P. J.; Wasielewski, M. R. *J. Am. Chem. Soc.* **2001**, *123*, 2440.

[6] Gregg, B. A.; Cormier, R. A. *J. Am. Chem. Soc.* **2001**, *123*, 7959.

[7] Breeze, A. J.; Salomon, A.; Ginley, D. S.; Gregg, B. A.; Tillmann, H.; Horhold, H. H. *Appl. Phys. Lett.* **2002**, *81*, 3085.

[8] Angadi, M. A.; Gosztola, D.; Wasielewski, M. R. *Mater. Sci. Eng. B* **1999**, *63*, 191.

[9] Ranke, P.; Bleyl, I.; Simmerer, J.; Haarer, D.; Bacher, A.; Schmidt, H. W. *Appl. Phys. Lett.* **1997**, *71*, 1332.

[10] Würthner, F. *Chem. Commun.* **2004**, 1564.

[11] Langhals, H. *Heterocycles* **1995**, *40*, 477.

[12] Langhals, H.; Demmig, S.; Huber, H. *Spectrochim. Acta.* **1988**, *44A*, 1189.

[13] Böhm, A.; Arms, H.; Henning, G.; Blaschka, P. Ger. Patent 19547209 A1, 1997; *Chem. Abstr.* **1997**, *127*, 96569g.

[14] Böhm, A.; Arms, H.; Henning, G.; Blaschka, P. Ger. Patent 19547210 A1, 1997; *Chem. Abstr.* **1997**, *127*, 96570a.

[15] Ahrens, M. J.; Fuller, M. J.; Wasielewski, M. R. *Chem. Mater.* **2003**, *15*, 2684.

[16] Zhao, Y.; Wasielewski, M. R. *Tetrahedron Lett.* **1999**, *40*, 7047.

[17] Lukas, A. S.; Zhao, Y.; Miller, S. E.; Wasielewski, M. R. *J. Phys. Chem. B* **2002**, *106*, 1299.

[18] Ma, Y.; Wang, C.; Zhao, Y.; Yu, Y.; Han, C.; Qiu, X.; Shi, Z. *Supramol. Chem.* **2007**, in press.

[19] Würthner, F.; Stepanenko, V.; Chen, Z.; Saha-Moller, C. R.; Kocher, N.; Stalke, D. *J. Org. Chem.* **2004**, *69*, 7933.

[20] Ego, C.; Marsitzky, D.; Becker, S.; Zhang, J.; Grimsdale, A. C.; Müllen, K.; MacKenzie, J. D.; Silva, C.; Friend, R. H. *J. Am. Chem. Soc.* **2003**, *125*, 437.

[21] Chen, S.; Liu, Y.; Qiu, W.; Sun, X.; Ma, Y.; Zhu, D. *Chem. Mater.* **2005**, *17*, 2208.

[22] Würthner, F.; Thalacker, C.; Diele, S.; Tschierske, C. *Chem. Eur. J.* **2001**, *7*, 2245.

[23] Würthner, F.; Thalacker, C. Ger. Patent 10039232 A1, 2000; *Chem. Abstr.* **2002**, *136*, 185323.

[24] Salbeck, J.; Kunkely, H.; Langhals, H.; Saalfrank, R. W.; Daub, J. *Chimia* **1989**, *43*, 6.

[25] Guldi, D. M.; Luo, C.; Swartz, A.; Gómez, R.; Segura, J. L.; Martín, N. *J. Phys. Chem. A* **2004**, *108*, 455.

[26] Yamanaka, K.; Fujitsuka, M.; Araki, Y.; Ito, O.; Aoshima, T.; Fukushima, T.; Miyashi, T. *J. Phys. Chem. A* **2004**, *108*, 250.

[27] Qu, J.; Pschirer, N. G.; Liu, D.; Stefan, A.; De Schryver, F. C.; Müllen, K. *Chem. Eur. J.* **2004**, *10*, 528.

[28] Allard, E.; Cousseau, J.; Ordúna, J.; Garín, J.; Luo, H.; Araki, Y.; Ito, O. *Phys. Chem. Chem. Phys.* **2002**, *4*, 5944.

[29] Kodis, G.; Liddell, P. A.; de la Garza, L.; Moore, A. L.; Moore, T. A.; Gust, D. *J. Mater. Chem.* **2002**, *12*, 2100.

[30] Wang, W.; Han, J.; Wang, L.; Li, L.; Shaw, W.; Li, A. D. Q. *Nano lett.* **2003**, *3*, 455.

[31] Langhals, H.; Ismael, R.; Eur *J. Org. Chem.* **1998**, 1915.